INT. J. NUM. METH. HEAT FLUID FLOW, VOL. 5, 327–340 (1995)

AN EFFICIENT BEM SOLUTION FOR THREE-DIMENSIONAL TRANSIENT HEAT CONDUCTION

ANIL GUPTA†, JOHN M. SULLIVAN, JR.† AND HUGO E. DELGADO‡

† *Mechanical Engineering Department, Worcester Polytechnic Institute, Worcester, MA, USA*
‡ *Wyman Gordon Company, North Grafton, MA, USA*

ABSTRACT

This paper presents a computationally efficient numerical solution scheme to solve transient heat conduction problems using the boundary element method (BEM) without volume discretization. Traditionally, a transient solution using BEM is very computer intensive due to the excessive numerical integration requirements at each time increment. In the present work a numerical solution scheme based on the separation of time and space integrals in the boundary integral equation through the use of an appropriate series expansion of the integrand (incomplete gamma function) is presented. The space integrals are evaluated only once in the beginning and within each time increment the additional integrals are obtained from the previously evaluated space integrals by a simple calculation. Three-dimensional applications are provided to compare the proposed strategy with that used traditionally. The CPU requirements are reduced substantially. The solution scheme presented allows for dynamically changing the time step size as the solution evolves. This feature is not practical in the traditional schemes based on boundary discretization only.

KEY WORDS Boundary element Transient Heat conduction Series expansions

INTRODUCTION

The boundary element method (BEM) has been shown to be an accurate, computationally efficient and robust numerical solution for certain classes of engineering problems[1]. The main advantage of BEM is in the areas of linear and steady state systems. Traditionally, transient analysis using BEM[2] has been extremely computer intensive such that its merits over the dominant numerical strategy, the finite element method (FEM), are compromised significantly. However, we present a transient BEM solution that retains the accuracy, boundary discretization only, and other advantages of the boundary element method without excessive computational effort normally required in a transient situation.

Consider the basic differential governing equation for heat conduction in a domain Ω, without internal heat sources or sinks:

$$\nabla \cdot k \nabla u(x, t) - \rho c_p \frac{\partial u(x, t)}{\partial t} = 0, \quad x \in \Omega \tag{1}$$

where k is thermal conductivity, ρ is density and c_p is specific heat at constant pressure of the solid. The temperature field u is a function of time and space. Assuming k to be independent of

0961–5539/95/040327–14$2.00

Received July 1993
Revised March 1994

space and denoting diffusivity by $K\ [=k/(\rho c_p)]$ we obtain:

$$\nabla^2 u(x, t) - \frac{1}{K}\frac{\partial u(x, t)}{\partial t} = 0 \tag{2}$$

with appropriate initial and boundary conditions.

The weighted residual integral representation of (2) for BEM can be presented in various forms. An early integral formulation was proposed in 1970 by Rizzo and Shippy[3]. The integral equation was formulated by taking the Laplace transform of (2) and writing the weighted residual statement on the transformed equation. The resulting equation was solved numerically, as was the transform inversion. Another BEM formulation of (2) approximated the time derivative in a finite difference form before writing the weighted residual statement[1]. Chang, Kang and Chen[4] formulated the integral equation by directly incorporating the differential equation in the weighted residual statement and integrating with respect to time and space. The time and space integrals were integrated using shape functions as in FEM. However, the time integral of the fundamental solution was carried out analytically which made the formulation less sensitive to time step size. The finite difference treatment of the temporal domain allows the user to march through time. To obtain the solution at time step $k+1$ the values of u at time step k are known and are used as initial conditions. Unfortunately, this requires domain and boundary discretizations which strips away one of the key assets of the boundary element method. Alternatively, integrating (2) in time and space and using an initial condition at $t=0$ for each increment of time step one can retain the reduced dimensional advantage of the BEM technique. Albeit, excessive storage and computational efforts are required to achieve the reduced dimensionality. We review briefly this solution strategy for ease of discussion in the following sections.

Consider the weighted residual statement of (2), i.e.:

$$\int_{t_o}^{t_F}\int_{\Omega}\left[\nabla^2 u(x, t) - \frac{1}{K}\frac{\partial u(x, t)}{\partial t}\right] u^*(\xi, x, t_F, t)\, d\Omega(x)\, dt = 0 \tag{3}$$

where $u^*(\xi, x, t_F, t)$ is the fundamental solution due to a point source placed at (t_F', ξ) in the time-space domain with t_F being the final time. The fundamental solution is of the form:

$$u^* = \frac{1}{(4\pi K\tau)^{3/2}}\, e^{-(r^2/4K\tau)} H(\tau) \tag{4}$$

where $\tau = t_F - t$ and

$$\begin{aligned} H(\tau) &= \text{Heaviside function} \\ &= 0 \quad t > t_F \\ &= 1 \quad t < t_F \end{aligned}$$

The fundamental solution satisfies the following properties:

$$\nabla^2 u^* + \frac{1}{K}\frac{\partial u^*}{\partial t} = -\delta(\xi, x)\delta(t_F, t) \tag{5}$$

and

$$\lim_{t \to t_F} u^*(\xi, x, t_F, t) = \delta(\xi, x) \tag{6}$$

By integrating (3) twice with respect to space and once with respect to time followed by collocation at the boundary the governing equation can be expressed as:

$$C(\xi)u(\xi, t_F) + K\int_{t_o}^{t_F}\int_{\Gamma} u(x, t) q^*(\xi, x, t_F, t)\, d\Gamma(x)\, dt = K\int_{t_o}^{t_F}\int_{\Gamma} q(x, t) u^*(\xi, x, t_F, t)\, d\Gamma(x)\, dt + \int_{\Omega} u_0(x, t_0) u^*(\xi, x, t_F, t_0)\, d\Omega(x) \tag{7}$$

where $C(\xi)$ is a function of the solid angle of the boundary at collocation point ξ, and $u_0(x, t_0)$ is the initial temperature field at $t = t_0$. The integral on the left is to be evaluated in the sense of Cauchy Principal Value. The normal gradient of the fundamental solution is denoted by q^*, where:

$$q^*(\xi, x, t_F, t) = \frac{\partial u^*(\xi, x, t_F, t)}{\partial n(x)}$$

The time variations of unknowns $u(x, t)$ and $q(x, t)$ are not known a priori, thus a time stepping scheme is followed. One procedure in use solves for the unknowns at the current time increment by using the response at the previous increment as the initial condition and evaluating the last integral of (7). This procedure involves volume discretization similar to the finite difference strategy[1] which takes away a fundamental feature associated with BEM. An alternate approach does not require volume discretization if the initial temperature field satisfies Laplace's equation. If the initial field is not Laplacian the latter approach is still valid but requires a volume integral at the initial time only[1]. Unfortunately, the solution at the current time step requires the boundary responses of all previous time steps since the volume integral vanishes only at the initial time (Laplacian). This procedure is more accurate than the scheme involving volume integration, but computationally inefficient. As a consequence, Chaudouet[5] recommended use of the volume integral procedure. However, we present a time stepping scheme that does not require volume integration, retains accuracy and is computationally efficient. The time and space effects are separated within the integration kernels. Therefore, the spatial integration is performed just once at the onset and saved in the form of coefficients. As time increases the integrated quantities are simply obtained by multiplying the spatial coefficients with the appropriate time constants at the new time. Thus the recomputation of spatial integrals with change in time is avoided.

NUMERICAL DISCRETIZATION

The governing equation (7) is discretized for the time-space domain. The time integral from initial time t_0 to final time t_F is divided into a series of time steps. Within each time step the unknowns u and q are assumed to have spatial variation only. The spatial integration uses quadratic isoparametric boundary elements (six noded triangular and/or eight noded quadrilateral). Discretizing (7) for constant time steps (total F), quadratic space variation for each element (total L) and using predetermined integration points[6] (number denoted by G, and is a function of collocation point ξ and element l) with weight W, we get:

$$C(\xi)u^F(\xi) + K \sum_{f=1}^{F} \sum_{l=1}^{L} \sum_{g=1}^{G_{gl}} \sum_{n=1}^{6\text{ or }8} \left(N_n W_g |J| \int_{t_{f-1}}^{t_f} q^*(\xi_i, x_j, t_F, t)dt \right) u_{ln}^f$$
$$= K \sum_{f=1}^{F} \sum_{l=1}^{L} \sum_{g=1}^{G_{gl}} \sum_{n=1}^{6\text{ or }8} \left(N_n W_g |J| \int_{t_{f-1}}^{t_f} (\xi_i, x_j, t_F, t)dt \right) q_{ln}^f \quad (8)$$

Integrating analytically the time integrals for u^* and q^* results in:

$$\int_{t_{f-1}}^{t_f} q^*(\xi_i, x_j, t_F, t)dt = \frac{d}{2\pi^{3/2} K r^3} \left[\Gamma\left(\frac{3}{2}, a_{f-1}\right) - \Gamma\left(\frac{3}{2}, a_f\right) \right] \quad (9)$$

and

$$\int_{t_{f-1}}^{t_f} u^*(\xi_i, x_j, t_F, t)dt = \frac{1}{4\pi^{3/2} K r} \left[\Gamma\left(\frac{1}{2}, a_{f-1}\right) - \Gamma\left(\frac{1}{2}, a_f\right) \right] \quad (10)$$

where $\Gamma(\ )$ is an incomplete gamma function (IGF)[7], d is $r(\xi_i, x_j) \cdot n(x_j)$, and $a_f = r^2/(4K[t_F - t_f])$ is a nondimensional parameter relating system length to the diffusional length. In matrix form

(8) can be written as:

$$\sum_{f=1}^{F} [H]_{fF}[u]_f = \sum_{f=1}^{F} [G]_{fF}[q]_f \tag{11}$$

After assembling for known and unknown quantities equation (11) results in:

$$[A]_{FF}[x]_F = [b]_F - \sum_{f=1}^{F-1} ([H]_{fF}[u]_f - [G]_{fF}[q]_f) \tag{12}$$

where $[x]_F$ are unknown u and q values for the time step F. At each time step all the $[H]$ and $[G]$ matrices for time steps $f = 1, 2, \ldots, F-1$ are recovered from storage and multiplied by the corresponding u_f and q_f vectors to form the right hand side vector at time F. Since matrix $[A]$ remains unchanged for each time step it can be factored once and saved for future use[8]. At every time step a new set of matrices $[H]_{1F}$ and $[G]_{1F}$ are required since the IGF differs in time for a constant r. Thus F time steps involve computation of F set of matrices; a computationally intensive exercise lacking practicality.

CONVENTIONAL SOLUTION SCHEME

In order to appreciate the proposed modification in the time stepping scheme, the conventional solution scheme and the associated computer expense is briefly described below.

(1) The conventional time stepping scheme involves construction (integration) of new $[H]$ and $[G]$ matrices at each time step. The matrices primarily involve the integration of IGF (a regular function of distance r) for every collocation point-element, combination pair. The truncated series expansion of the IGF is evaluated at each Gauss integration point. The order of Gauss quadrature used is a function of the number of terms retained in the series expansion. The integration, although regular, is very computationally intensive.
(2) All the matrices generated prior to the current time are required to be stored on disk, thus requiring an enormous amount of disk space for a reasonably large practical problem.
(3) The right-hand side vector of (12) uses all the previously stored matrices. This results in extensive I/O operations at each time step.
(4) The time step size must remain constant throughout the analysis. The analysis is forced to proceed at a uniform rate even if the response warrants a change in time step size. Any change in time step size requires regeneration of all the $[H]$ and $[G]$ matrices up to the current time. This effort is not practical.

PROPOSED SOLUTION SCHEME

The following section suggests a modification in the solution strategy of (12), described above. The governing equation (8) involves interrelated time and space integrals. If the two effects (time and space) can be separated then as time advances only the time integral will change. The space integral does not change because the geometry is not deforming appreciably to call for updating (small deformation).

The time effects are present in the analytical integration of u^* and q^* as in (9), (10). The IGF includes the time effects. Using an appropriate truncated series expansion of the IGF the time and space effects can be separated. Selecting the IGF as a confluent hypergeometric function[7] gives the desired result. The space integration corresponding to each term of the series expansion can be carried out accurately once and saved. The successive matrices $[H]$ and $[G]$ for each time step can be computed very efficiently by simply retrieving the spatially integrated terms (stored) and multiplying with the new time constant.

In order to demonstrate the separation of space and time variables, the first few terms of the series expansion are shown below:

$$\Gamma\left(\frac{1}{2}, a_f\right) = \Gamma\left(\frac{1}{2}\right) - 2\left[\left(\frac{r^2}{4K}\right)^{1/2} \frac{1}{(\Delta t_f)^{1/2}} - \left(\frac{r^2}{4K}\right)^{3/2} \frac{1}{3(\Delta t_f)^{3/2}} + \left(\frac{r^2}{4K}\right)^{5/2} \frac{1}{10(\Delta t_f)^{5/2}} - \cdots\right]$$

where $\Delta t_f = t_F - t_f$. A similar expression is obtained for $\Gamma(\frac{3}{2}, a_f)$. In concise form, we can write:

$$\Gamma(\tfrac{1}{2}, a_f) = C - F1(r)\Delta t_f^{-1/2} + F2(r)\Delta t_f^{-3/2} + F3(r)\Delta t_f^{-5/2} - \cdots \tag{13}$$

Functions $F1, F2, F3, \ldots$ depend only on the spatial variable r. Also, the Jacobian of the element and the shape function values at an integration point are a function of the geometry of the element being integrated. Thus the product of all the spatial quantities can be integrated once and saved during the computation of the first set of $[H]$ and $[G]$ matrices. To generate the subsequent matrices $[H]_{1F}$ and $[G]_{1F}$ as time progresses, only time difference Δt_f changes, thus the stored spatial quantities are retrieved and multiplied by the new Δt_f constants. It is to be noted that integration is not required to generate these new set of matrices.

In this paper the series expansion for the IGF is truncated at twenty terms or less (a_f dependent). *Table 1* compares the exact IGF values with the approximate values for various cut-off values of a_f and the number of terms retained in the series expansion.

The three most important consequences of the separated time and space integrals are:

(1) For each time step, the required $[H]_{1F}$ and $[G]_{1F}$ matrices are generated by multiplying the previously computed spatial coefficients with the new time constants.
(2) Time steps are not required to be constant in size. The new matrices from the changed time step size to the initial time are regenerated easily from the spatial coefficients, the only change is in time constants.
(3) In the present formulation the value of IGF is approximately zero for $a_f > 5.5$. Thus for a particular size of time step, there is a maximum distance from a collocation point beyond which the kernel is assumed zero. This results in a banded structure and specialized banded solvers can be used.

DISK STORAGE REQUIREMENT

The disk storage with the proposed scheme can be constant or variable depending on its availability. The constant option uses the minimum storage (i.e. storage for a maximum of twenty coefficients for each collocation point-element combination), whereas the variable option

Table 1 Comparison of incomplete gamma functions with finite terms of series expansion

a_f ≤	Number of terms in series	$\Gamma(\frac{1}{2}, a_f)$		$\Gamma(\frac{3}{2}, a_f)$	
		Exact	Approx.	Exact	Approx.
0.0	1	1.7724	1.7724	0.8862	0.8862
1.2	5	0.2151	0.2115	0.4374	0.4339
1.3	6	0.1895	0.1904	0.4054	0.4066
1.7	7	0.1156	0.1144	0.2960	0.2942
1.9	8	0.0908	0.0914	0.2516	0.2526
2.2	9	0.0637	0.0633	0.1962	0.1953
2.3	10	0.0567	0.0568	0.1804	0.1807
3.1	12	0.0226	0.0228	0.0906	0.0912
4.4	15	0.0053	0.0050	0.0284	0.0269
5.5	20	0.0016	0.0016	0.0104	0.0105

sacrifices storage economy (storage for $[H]$ and $[G]$ matrices for all time steps) in favour of computational time reductions.

The constant storage option is ideal for limited disk space availability. At every new time increment all the previous matrices are regenerated, very efficiently, from the stored spatial coefficients to generate the right hand vector in (12). (Ideally suited for vector computers.) The minimum storage, with the constant option, is a constant value, whereas the storage for the conventional scheme depends on the number of time steps in the analysis (thus has no upper bound on the disk storage requirements). Therefore, after a critical number of time steps the disk storage for the conventional scheme will exceed that required for the proposed scheme (Examples 1 and 3 show a saving in the disk usage with an increase in the number of time steps).

The variable option is activated in the presence of sufficient disk space. A new set of $[H]$ and $[G]$ matrices generated (from stored twenty spatial coefficients) at each time increment are also stored on the storage device for use in the subsequent analysis. Therefore, the storage required for this option will always exceed that required for the conventional scheme. Nevertheless, this option results in further saving in the computation time by avoiding the regeneration of all the matrices at each time increment associated with the constant disk storage option (Examples 1 and 3 show the CPU advantage with this option).

INTEGRATION

Singular integration

The integration kernel for the first set of $[H]$ and $[G]$ matrices are singular in nature. The order of singularities for $[H]$ and $[G]$ are $1/r^2$ and $1/r$, respectively, as is evident from (9), (10). For the first time step ($t_f = t_F$), a_f goes to infinity and $\Gamma(3/2, a_f) = \Gamma(1/2, a_f) = 0$.

Singularity of order $1/r$ is a weak singularity and is removed by integrating the differential element using polar coordinates. The Jacobian of transformation from Cartesian to polar coordinates is of order r which cancels the singularity of the integrand. The singularity of the form $1/r^2$ is a strong singularity and exists in the sense of Cauchy principal value. This singularity is of the same form as that present in the steady state heat transfer analysis[1,9]. Thus, an indirect procedure can be used to compute the singular terms as well as the free term using the concept of constant temperature field giving rise to a zero flux condition. Appendix A describes in detail the separation of the singularity and the indirect procedure used to evaluate it.

Non-singular integration

Non-singular kernels require integration for the first set as well as all subsequent sets of $[H]$ and $[G]$ matrices. For the first set the order of subsegmented Gauss quadrature required is an inverse function of the relative distance r between the collocation point and the element being integrated[6], and a direct function of powers of r appearing in the series expansion of IGF. The subsequent sets are only a function of the highest power of r in the series expansion. Since a_f decreases as time progresses (for a particular element and the collocation point) the accuracy of first integration set implies that all subsequent matrices generated from the spatial coefficients of the first set will increase in accuracy. Alternately, to retain approximately the same accuracy for the subsequent matrices fewer coefficients can be used to form new matrices (*Table I*).

As shown in *Table I*, the truncated series expansion of IGF gives a good approximation for $a_f \leqslant 5.5$. Beyond this value the IGF is approximately zero. The proposed solution scheme assumes a zero value for $a_f > 5.5$. Because of this jump in the numerical implementation of the series expansion, three different integration cases based on the position of the element spanning the cut-off point are recognized. *Case (i)* – Element lies completely in the region defined by $a_f > 5.5$, *Case (ii)* – Element spans the cut off point ($a_f = 5.5$), and *Case (iii)* – Element is completely in the region $0 < a_f < 5.5$.

Case (i) – The contribution to the Boundary Integral Equation due to this element is insignificant. Since the coefficient matrix is diagonally dominant, the solution will not be disturbed appreciably because of this insignificant contribution. An appreciable saving is achieved by totally ignoring this element. This strategy results in a banded structure for $[A]_{FF}$ in (12) which leads to further savings in factorization, and forward and backward substitution steps for each time step. Also, only the banded structure need be stored. As time advances, the a_f for this element decreases and its classification may change to *Case (ii)* and/or *Case (iii)*. Thus the movement of the element is monitored. In fact the exact time step when the element enters the significant range ($0 < a_f \leqslant 5.5$) can be computed at the beginning.

Case (ii) – Elements of this category span the a_f cut-off line. This case requires a separate integration for the collocation point-element-time step(s) combination. Previously computed coefficients cannot be used to compute the integration for this case. This is the only situation wherein a separate integration apart from integration in the first time step is required. This case will not occur for an element already in the region of *Case (iii)*, as the element only moves to the left (a_f decreases) with time.

Case (iii) – Element is completely within the $0 < a_f \leqslant 5.5$ region. Once an element has entered the region for this case, it will remain in the region for all subsequent time steps. The spatial coefficients once formed can be used to generate subsequent matrices.

NUMERICAL EXAMPLES

Three examples are presented to demonstrate the efficiency of the present solution scheme. The CPU timings reported herein are taken from the Encore Multimax computer at Worcester Polytechnic Institute (WPI). The processing speed of Encore computer is approximately 7 MIPS/CPU. The thermal diffusivity K used for these three-dimensional examples is 0.125 m^2/s.

Example 1 – Sudden heating of a cube

A unit cube initially at a zero temperature is suddenly heated on the top face such that a temperature of 100°F is maintained for $t > 0$. All the other faces are thermally insulated. The time-temperature history is studied at the base of the cube (*Table 2*). The analytical solution presented in Reference 10 is used to evaluate the numerical solution. The BEM mesh used for this analysis has only one element (8-noded quadratic) in the flow direction (*Figure 1*). Even

Table 2 Time–temperature history at the base of a cube heated suddenly at the top

Time elapsed (s)	Analytic (°F)	Numerical (°F)	
		$\Delta t = 0.4$	$\Delta t = 0.2$
0.8	5.07	4.05	4.34
1.6	22.77	21.54	21.90
2.4	39.32	38.77	38.86
3.2	52.55	52.56	52.46
4.0	62.92	63.23	63.05
4.8	71.03	71.46	71.26
5.6	77.36	77.79	77.64
6.4	82.31	82.68	82.58
7.2	86.18	86.45	86.40
8.0	89.20	89.36	89.37
8.8	91.56	91.62	91.68
9.6	93.41	93.37	93.47

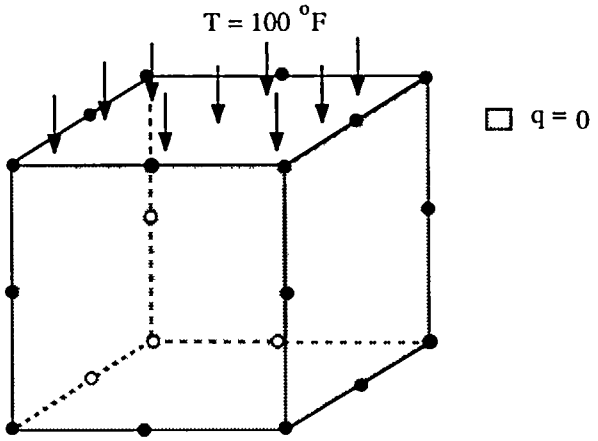

Figure 1 A unit cube with zero initial temperature and the top surface maintained at a constant temperature of 100°F for $t > 0$

with such a coarse mesh BEM gives a reasonably good result. This example is also solved by Dargush and Banerjee[9], wherein they report similar results. *Table 2* shows the BEM results for two different constant time step sizes. The convergence of the result with decreasing time step size is evident.

Table 3 compares the CPU and the disk storage requirements (both constant and variable option) with and without the proposed modification of the solution scheme. The requirement of disk storage is measured in megawords (MW).

The analysis was carried out twice to a total elapsed time of 10 seconds using 25 and 50 time steps, respectively. The CPU required for the conventional solution scheme is estimated based on the time taken to generate first set of matrices. Without modification each subsequent matrix is generated by integrating the non-singular kernels (higher order in r). In this work the CPU time required (on average) for each additional set of matrices has been estimated as 1/4 of that needed to generate first set of matrices.

Example 2 – Thick casing around a current carrying wire

A long casing for a current carrying wire is analyzed to demonstrate the applicability of the proposed modification for multizone BEM. A twenty zone model of a small segment of the casing (neglecting curvature), 20 m long is considered (*Figure 2*). Each zone is a unit cube and has six 8-noded quadratic isoparametric boundary elements. The model has a total of 248 nodes. The inside of the casing is subjected to a constant heat flux of 100 W/m^2. The outside face is maintained at zero temperature for $t > 0$. The casing was initially at zero temperature.

A multizone analysis in BEM is preferred due to a substantial saving in CPU and disk storage requirements. But, unfortunately, the computer code to properly account for multi-zones is complex and cumbersome. Moreover, the multizone solution is, in general, somewhat less accurate than the corresponding single zone solution due to the need for additional modelling of the responses at the interfaces. But the advantage gained in CPU and the storage requirements outweighs this slight reduction in accuracy.

In many practical situations one is only interested in the transient response in a narrow time range beyond the onset. In such situations, the proposed solution scheme applied to a single zone model can match the CPU and the storage requirements of a multi-zone model coupled with the improved accuracy of the single zone solution. As time advances the range of influence of each node in a single zone model increases and new elements have to be added to the

Table 3 CPU and disk storage requirements for a cube heated suddenly at the top
Nodes = 20; Elements = 6

Time step size (s)	Number of time steps	CPU required to form matrices [G] and [H] (s)			Disk storage (MW)			Total CPU used (s)		
		First set	Each additional set		PM		WPM	PM		WPM (estimated)
			PM (average)	WPM (estimated average)	I	II		I	II	
$\Delta t = 0.4$	25	146	0.57	36.5	0.0384	0.0584	0.020	330	160	1022
$\Delta t = 0.2$	50	146	0.34	36.5	0.0384	0.0784	0.040	559	163	1935

PM, proposed modification; I, constant disk storage; II, variable disk storage
WPM, without proposed modification
Note: Disk I/O operations are not accounted for in the CPU timings

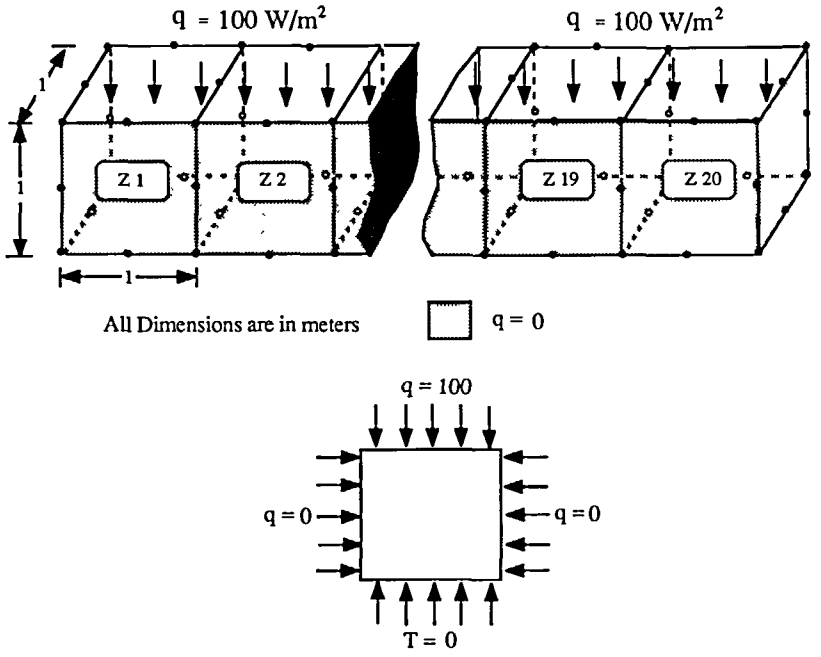

Figure 2 A twenty zone model of a long thick casing around a current carrying wire

Table 4 Temperature profile at inside of a thick casing around a current carrying wire

Time elapsed (s)	Analytic (°F)	Numerical (°F) $\Delta t = 0.4$ Number of zones 1	20
0.0	0.00	0.00	0.00
0.4	201.85	201.89	201.97
0.8	285.46	286.74	288.31
1.2	349.56	352.22	355.58
1.6	403.27	406.90	411.75
2.0	449.79	453.90	459.88

integration. As a result, the single zone analysis demands more CPU with increasing time, whereas a multizone analysis remains at the same level.

The proposed scheme is applied to a multi-zone and a single zone model of the wire casing, and the solutions compared. A single zone analysis of the casing with the proposed modification results in a banded structure with a half bandwidth of 23. (Bandwidth is time step dependent, $\Delta t = 0.4$ in the present study.) The analysis is carried out to a total elapsed time of 2 seconds. The requirements of CPU and disk storage for a single zone analysis are nearly the same as for the multizone analysis for this short time range. *Table 4* depicts the temperature profile at the

inside of the casing for a single zone and twenty zone BEM model. A somewhat improved result of the single zone response is evident. The analytical solution is obtained from Reference 10.

Example 3: Spherical inclusion in an infinite domain

The transient response due to a constant flux of 12.5 W/m^2 for $t > 0$ at the surface of a spherical inclusion of unit radius in an infinite domain is studied. The infinite domain was at zero temperature at $t = 0$. The BEM mesh for this example is only a model of the spherical inclusion. The boundary at infinity does not enter into the formulation as the response vanishes at infinity. Two refinements of BEM model are used to show the convergence of the proposed solution scheme with respect to time step size. The analytical solution is from Reference 10. An octant of the inclusion is shown in *Figure 3a–b*. *Table 5* shows the convergence of the transient temperature profiles at the spherical inclusion for both boundary meshes.

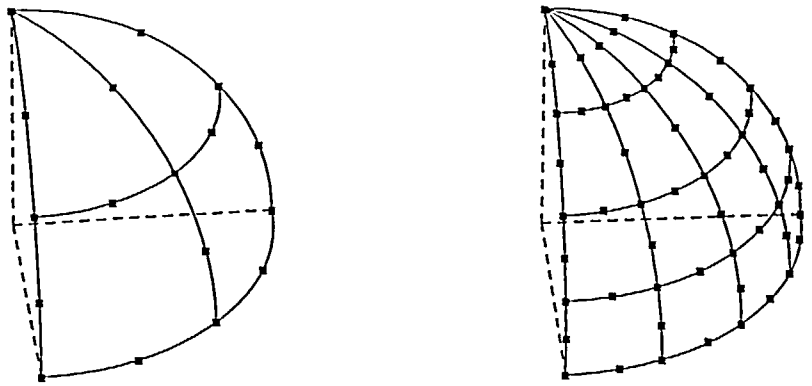

Figure 3 An octant of a spherical inclusion of unit radius in an infinite domain. The number of elements/octant are: (a) four; (b) sixteen

Table 5 Transient temperature profile at a spherical inclusion of unit radius in an infinite domain

Time elapsed (s)	Analytic (°F)	Numerical (°F)			
		Boundary elements/octant			
		4		16	
		$\Delta t = 1.0$	$\Delta t = 0.5$	$\Delta t = 1.0$	$\Delta t = 0.5$
0.0	0.00	0.00	0.00	0.00	0.00
2.0	38.43	35.83	36.38	36.54	37.12
4.0	47.68	45.65	46.07	46.37	46.81
6.0	53.28	51.64	51.94	52.37	52.68
8.0	57.24	55.84	56.06	56.57	56.81
10.0	60.26	59.00	59.18	59.74	59.93
12.0	62.68	61.52	61.66	62.26	62.41
14.0	64.68	63.58	63.70	64.34	64.46
16.0	66.38	65.32	65.42	66.09	66.19
18.0	67.84	66.82	66.90	67.59	67.68
20.0	69.12	68.12	68.20	68.90	68.98

Table 6 CPU and disk storage requirements for a spherical inclusion of unit radius in an infinite domain
Nodes = 82; Elements = 32

Time step size (s)	Number of time steps	CPU required to form matrices [G] and [H] (s)			Disk storage (MW)			Total CPU used (s)		
			Each additional set							
				WPM	PM			PM		
		First set	PM (average)	(estimated average)	I	II	WPM	I	II	WPM (estimated)
$\Delta t = 1.0$	40	700	2.2	175	0.840	1.378	0.538	2416	786	7525
$\Delta t = 0.5$	80	700	2.1	175	0.840	1.916	1.076	7336	866	14525

PM, proposed modification; I, constant disk storage; II, variable disk storage
WPM, without proposed modification
Note: Disk I/O operations are not accounted for in the CPU timings

Table 7 Variable time step for a spherical inclusion in an infinite domain

Time elapsed (s)	Analytic (°F)	Numerical (°F) Time step size: Constant $\Delta t = 1.0$	Numerical (°F) Time step size: Variable $\Delta t = 1.0$
5.0	50.76	48.95	48.95
		$\Delta t = 1.0$	$\Delta t = 1.5$
11.0	61.54	60.33	60.22
17.0	67.14	66.10	66.03
23.0	70.77	69.81	69.76
29.0	73.39	72.46	72.42
35.0	75.41	74.49	74.46
	CPU used	2000	1400
			Saving = 30%

We use this example with the coarser mesh to highlight two features of the proposed BEM strategy. First, the CPU expense is reduced substantially compared to the conventional solution methodology. Second, the proposed strategy demonstrates the ability to change the time step size dynamically without incurring CPU penalties.

Table 6 shows the disk storage and CPU savings realized from the proposed scheme with both constant and variable disk storage requirements. Again, the CPU time for the conventional solution scheme to generate each additional set of matrices is assumed to be 1/4 of that required for the first set. The conventional scheme has massive CPU requirements such that a timely response becomes unobtainable.

Finally the feasibility of using variable time step size is illustrated within the proposed solution scheme framework. *Table 7* shows the analysis results for the coarse BEM model for a time step size of 1 and 1.5 seconds. A change of time step size is called for after a total time of 5 seconds as the response is not changing rapidly after the initial 5 seconds. A saving of 30% in CPU time is achieved without loss of accuracy. The time step size must remain constant for the conventional solution scheme.

CONCLUSION

This paper presented an efficient numerical strategy for the solution of transient heat transfer problems using BEM without volume discretization. The numerical efficiency in terms of CPU expense is achieved through the separation of space and time effects in the incomplete gamma functions. Since the spatial quantities do not change with time, integration is required only at the initial time. The temporal quantities at a particular time step are obtained simply by computation of precomputed, and stored coefficients. The numerical results show a substantial saving in computer resources without loss of accuracy.

REFERENCES

1 Brebbia, C. A., Telles, J. C. F. and Wrobel, L. C. *Boundary Element Techniques*, Springer-Verlag (1984)
2 Wrobel, L. C. and Brebbia, C. A. Time dependent potential problems, Chapter 6 in *Progress in Boundary Element Methods*, Pentech Press, London (1981)

3 Rizzo, F. J. and Shippy, D. J. A method of solution for certain problems of transient heat conduction, *AIAA J.*, **8**, 2004–2009 (1970)
4 Chang, Y. P., Kang, C. S. and Chen, D. J. The use of fundamental Green's function for the solution of problems of heat conduction in anisotropic media, *Int. J. Heat Mass Transfer*, **16**, 1905–1918 (1973)
5 Chaudouet, A. Three-dimensional transient thermo-elastic analyses by the BIE method, *Int. J. Numer. Meth. Eng.*, **24**, 25–45 (1987)
6 Kane, J. H., Gupta, A. and Saigal, S. Reusable intrinsic sample point (RISP) algorithm for the efficient numerical integration of three dimensional curved boundary elements, *Int. J. Numer. Meth. Eng.*, **28**, 1661–1676 (1989)
7 Abramowitz, M. and Stegun, I. A. *Handbook of Mathematical Functions*, National Bureau of Standards, Applied Mathematics Series, 55, November 1964
8 Pina, H. L. G. and Fernandes, J. L. M. Applications in transient heat conduction, in *Topics in Boundary Element Research* (C. A. Brebbia, Ed.), Springer-Verlag (1984)
9 Dargush, G. F. and Banerjee, P. K. Boundary element method in three-dimensional thermoelasticity, *Int. J. Solids Structures*, **26**, 2, 199–216 (1990)
10 Carslaw, H. S. and Jaeger, J. C. *Conduction of Heat in Solids*, 2nd ed., Clarendon Press, Oxford (1959)

APPENDIX A

Computation of Cauchy integral in transient heat conduction

Consider the boundary integral equation for transient heat transfer analysis. The governing equation for the case of a constant initial condition where $u_0 = 0$ is:

$$C(\xi)u(\xi, t_F) + K\int_{t_o}^{tF}\int_{\Gamma} u(x, t)q^*(\xi, x, t_F, t)d\Gamma(x)dt = K\int_{t_o}^{tF}\int_{\Gamma} q(x, t)u^*(\xi, x, t_F, t)d\Gamma(x)dt \tag{A.1}$$

The strong singularity (which exist in the sense of Cauchy principal value) resides in the integral on the left. Discretization equation (A.1) for constant time steps and using (9)–(10) we obtain for the first time step:

$$C(\xi)u(\xi, t_F) + K\int_{\Gamma} u(x)\frac{d}{2\pi^{3/2}Kr^3}\left[\Gamma\left(\frac{3}{2}, a_{F-1}\right) - \Gamma\left(\frac{3}{2}, \infty\right)\right]d\Gamma(x)$$
$$= K\int_{\Gamma} q(x)\frac{1}{4\pi^{3/2}Kr}\left[\Gamma\left(\frac{1}{2}, a_{F-1}\right) - \Gamma\left(\frac{1}{2}, \infty\right)\right]d\Gamma(x) \tag{A.2}$$

The integral on the right is weakly singular and can be computed by an appropriate transformation. However, the left integral is strongly singular of $O(1/r^2)$ and requires special consideration.

The order of singularity is more explicit if the incomplete gamma function is expanded in an infinite series as in equation (13). Considering the left hand side of the above equation and substituting the series function $[C - F(r, K, t)$, where $C = \text{sqrt}(\pi)/2$, for $\Gamma(3/2, a_{F-1})]$ for the incomplete gamma function, we get

$$C(\xi)u(\xi, t_F) + K\int_{\Gamma} u(x)\frac{d}{2\pi^{3/2}Kr^3}\left[\frac{\sqrt{\pi}}{2} - F(r, K, t)\right]d\Gamma(x) \tag{A.3}$$

This implies:

$$C(\xi)u(\xi, t_F) + \int_{\Gamma} u(x)\frac{d}{4\pi r^3}d\Gamma(x) - K\int_{\Gamma} u(x)\frac{d}{2\pi^{3/2}Kr^3}F(r, K, t)d\Gamma(x) \tag{A.4}$$

The first integral of (A.4) is strongly singular in nature. The second integral (regular) tends to zero as time goes to infinity, indicating the convergence of the transient formulation to a steady state response. The first two terms of (A.4) are due to a steady state response and are evaluated indirectly by forcing the system of equations to satisfy the condition of a unit constant temperature field. This condition also results in a zero flux field on the boundary.